

## COB-2023-2161

### Modal analysis of SpectraQuest's Machinery Fault Simulator

**Luiz Felipe da Rosa Fonseca da Silva**

**Maria Vitoria Sikora**

**Luisa Yumi Antunes Kaneko**

**Júlio Cordioli**

**Danilo Braga**

Universidade Federal de Santa Catarina, Florianópolis - SC, 88040-900 - Brazil

luizffonseca4@gmail.com, maria.sikora@lva.ufsc.br, luisaantuneskaneko@gmail.com, julio.cordioli@ufsc.br, danilo@dynamox.net

**Abstract.** Predictive maintenance is generally recognized as the best maintenance strategy for most industries. Among the possibilities, vibration-based condition monitoring is considered the most cost-effective, due to its fast response to changes in the system. In order to study machinery fault vibration signals, several studies in the literature utilize SpectraQuest's Machinery Fault Simulator (MFS) – a test bench that emulates a machine and its elements. The measured vibration signal of a machine is a mixture of source effects and transmission path effects. Modal analysis is a tool that obtains a function to its transmission path. Therefore, the modal analysis of the MFS is a topic of interest. This article presents the Finite Element Method (FEM) and experimental modal analysis of SpectraQuest's Machinery Fault Simulator. It focuses on the bearing base, bearing support, C-shaped beam and the assembly of these components. Experimental tests were made with the assistance of BK Connect software. The individual components were excited with an impact hammer and the assembly with a shaker. The experimental results were used in order to adjust the FEM simulation, made with the COMSOL Multiphysics software, with parameters such as the material elasticity, density and damping. The numerical model is able to represent the analysed components of MFS's test bench.

**Keywords:** Modal Analysis, Machinery Fault Simulator, SpectraQuest, Predictive Maintenance.

#### 1. INTRODUCTION

Machines and equipment are susceptible to wear and, therefore, require maintenance. There are mainly three approaches to maintenance: corrective, preventive and predictive maintenance. Nowadays, predictive maintenance – which is based on monitoring a machine's condition – is recognized as the best strategy for the majority of the cases. It anticipates potential failures, is an effective cost-cutting method, eliminates unnecessary revisions and increases employee safety (Randall, 2011).

To monitor a machine's condition, a few parameters are used: temperature, particles in lubricant, acoustic emission and vibration. Although each one offers advantages and disadvantages, vibration-based condition monitoring stands out among them. It has fast response to changes and, since each component has its own vibration signature, it can detect local and type of defect (Randall, 2011). The work of (Tiboni *et al.*, 2022) finds that vibration-based condition monitoring detects of 90% of faults in the industry. Up to 4th of November, 2021, (Tiboni *et al.*, 2022) reports 957 published documents in the field of vibration-based condition monitoring of rotating machinery.

To gain understating on vibration behavior of machines there are a few devices that emulate real world machinery. One of them is the *Machinery Fault Simulator* (MFS) by SpectraQuest, showed in Fig. 1. (Mustafa and Nayfeh, 2020) review papers that employed the MFS. They reported 143 papers since 1998. From 2011 on, at least 12 papers per year were published. In 2019 alone 28 papers were produced. Further information can be found in (Mustafa and Nayfeh, 2020)'s article.



Figure 1. SpectraQuest's Machinery Fault Simulator. Source: (SpectraQuest, 2023)

Usually when machines operate at constant speed, peaks at the rotation of machine components and their harmonics appears at their vibration spectrum. One challenge of vibration-based condition monitoring is inferring if the change occurred at the source – such as modifications in the force between meshing gears –, in the structural transmission path – such as developing cracks – or both (Randall, 2011). The structural transmission path can be described by a Frequency Response Function (FRF), also called transfer function (Rao, 2010). It correlates input (excitation) and output (response) of a structure. A tool to find the FRF from a structure is modal analysis, which correlates force input with vibration output. A dynamic model of a structure is a powerful tool that simulates the response of a structure to any excitation in a given frequency range.

## 1.1 Objective

As aforementioned, the basic problem of vibration-based condition monitoring is inferring which response comes from the structural transmission path and which comes from the machine elements rotating excitation. SpectraQuest's MFS is commonly used test bench for vibration-based condition monitoring. Modal analysis is a tool that characterizes a system dynamically in the frequency domain. Given the importance of MFS to the growing predictive maintenance field, this paper objective is to present a modal analysis of the MFS. More specifically, it focuses on the following components: bearing base, bearing support, C-shaped beam and the assembly of these components.

## 2. LITERATURE REVIEW

Modal analysis is a tool to obtain models that represent the dynamics of structures, correlating force input and vibration output. Useful information found through modal analysis are: (a) natural frequencies, or the rate in which a structure vibrates naturally when disturbed, (b) mode shapes, or the deflection pattern associated with a given natural frequency, (c) damping information and (d) FRFs, which encompasses all of these information (Maia and Silva, 1997). Modal analysis can be done in different ways. Commonly, an experimental modal analysis, a.k.a. modal testing, is done, then to update a Finite Element Method (FEM) model.

According to (Ewins, 2009) modal testing is “*the processes involved in testing components or structures with the objective of obtaining a mathematical description of their dynamic or vibration behaviour*”. For the experimental modal analysis, several points to be measured are distributed along the structure, correlating force applied and displacement measured. The extent and quality of a modal testing increases in conjunction with the intended model's accuracy (Maia and Silva, 1997). The more points, the better the accuracy of the mode shapes.

The basic measurement chain of modal testing encompasses an excitation mechanism, a sensing mechanism and data acquisition and processing mechanism. The excitation mechanism is usually an impact hammer or a shaker. The impact hammer has a force transducer at its tip, measuring the force applied. The shaker needs to be connected to a force transducer by a stinger – a flexible rod that functions as a mechanical fuse. While the impact hammer has an easier mounting, the shaker usually provides higher coherence (consistency between measurements) and is better suited for large amounts of measuring points. To quantify the displacement along the structure points, accelerometers are typically applied. The sensors' signals are acquired and processed, then to obtain FRFs, natural frequencies, mode shapes and damping information.

Modal analysis can also be done by FEM. According to (Shabana, 2019), in summary, FEM consists of dividing a given continuous geometry into multiple elements. Each element is modeled as an individual object that connects to adjacent elements through nodes with a number of Degrees of Freedom (DoF). This network of nodes is called a mesh. For each element, we can describe deformations using interpolating polynomials. The coefficients of these polynomials are defined based on physical coordinates called element nodal coordinates, which represent the displacements and slopes at chosen nodal points within the element. From this mesh of nodes, stiffness, mass, and damping matrices of the structure are generated, which form a linear system of equations for the motion of the DoF described by Eq. (1),

$$\mathbf{M} \ddot{\mathbf{x}}(t) + \mathbf{C} \dot{\mathbf{x}}(t) + \mathbf{K} \mathbf{x}(t) = \mathbf{f}(t), \quad (1)$$

where  $\mathbf{M}$ ,  $\mathbf{C}$ , and  $\mathbf{K}$  are the mass, dissipation and stiffness matrices, respectively, and  $\ddot{\mathbf{x}}$ ,  $\dot{\mathbf{x}}$ ,  $\mathbf{x}$ , and  $\mathbf{f}$  are the acceleration, velocity, displacement, and input force vectors, respectively. Equation (1) shows a system with ordinary differential equations (ODE) which can be solved in two main ways: through modal analysis, which solves the eigenvalue and eigenvector problem to find the natural vibration modes of the system, and the direct method, which determines the system's response when excited by forces with defined amplitude and frequency at a set of nodes (Meirovitch, 2002). Since damped natural frequencies are similar to undamped for most structures, damping can usually be neglected at the analysis (Beards, 1996). Equation (2) shows the modal analysis for the undamped system:

$$\det(\mathbf{K} - \omega^2 \mathbf{M}) = 0. \quad (2)$$

The eigenvalues are the natural frequencies and the eigenvectors are the modes of the system (Petyt, 2010). Consider-

ing a proportional damping model, the FRF,  $\tilde{H}(\omega)$ , elements are described by Eq. (3):

$$\tilde{H}_{jk}(\omega) = \sum_{n=1}^N \frac{U_{jn}U_{kn}}{\omega_n^2 - \omega^2 + 2i\xi_n\omega_n^2\omega}, \quad (3)$$

where  $\omega$  represents frequency,  $U$  represent the eigenvectors obtained through modal analysis,  $U_{jn}$  is the  $j$ -th element of the  $n$ -th eigenvector, and  $j$  is the response DoF and  $k$  the excitation DoF. The natural frequency of a given mode is  $\omega_n$ , the damping coefficient of a given mode is  $\xi_n$  and  $N$  represents the total number of modes or natural frequencies.

### 3. METHODS

To obtain the dynamic response model of SpectraQuest's MFS, we divided the process into a few steps. Initially, we created a 3D model of the MFS at SolidWorks CAD software by measuring it with a pachymeter. This model served as the basis for conducting modal analysis simulations of each component in the assembly using the eigenfrequency method on the COMSOL Multiphysics software. These simulations with estimated material properties provided valuable insights and allowed us to optimize the setup and mesh for the subsequent experimental step.

The components to be analyzed are identified in Fig. 2. Component 1, highlighted in red, represents the bearing base. Component 2, shown in yellow, represents the bearing support, and Component 3, marked in blue, represents the C-shaped beam. Ultimately, modal analysis of the assembly comprising these components is also done.

To acquire the experimental data, we utilized the SW-3592 acquisition module that has a accuracy of  $\pm 0.1$  dB in conjunction with the BK Connect software, both from B&K. More details on the mesh and equipment of each component and assembly will be stated in their respective methods section. The results of the experimental modal analysis were employed to adjust the FEM model. The parameters (material density, Young modulus, damping ratio) were adjusted manually by comparison of experimental and simulated FRFs.

In the Finite Element Method (FEM) model, we employ tetrahedral elements within the mesh and gauge their quality through the average element skewness metric. This metric serves as an indicator of how closely each element approximates an equilateral (ideal) element. Equilateral elements significantly enhance accuracy by ensuring uniformly spaced nodes, thereby facilitating simulation convergence.

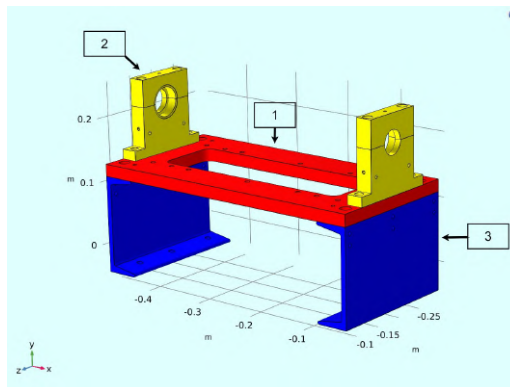


Figure 2. MFS modeled elements where (1) represents the bearing base (2) represents the bearing supports and (3) represents the C-shaped beam

#### 3.1 Bearing base

This section presents the experimental and numerical modal analysis methods of the bearing base.

##### 3.1.1 Numerical methods

To begin the modal analysis, in COMSOL Multiphysics software, we generated the mesh within the domain obtained through the CAD model. We employed the "Free Tetrahedral method" with the default size "finer" provided by COMSOL Multiphysics to generate the elements for the mesh. This configuration yielded an average element skewness of 0.655. The resulting mesh (Fig. 3.a) consisted of 89,225 elements and 19,177 nodes. For the boundary conditions, we set them to "Free", similar to the conditions used in the experimental analysis. To generate an FRF, a unitary harmonic punctual force in the point where the accelerometer was fixed. This FRF was used to compare with the experimental one, then to update material properties of the component. The study conducted the "Frequency domain modal analysis", where we configured the simulation to identify the first 18 modes, with a frequency range of 1-3000 Hz and a frequency resolution of 1 Hz.

### 3.1.2 Experimental methods

First, we designed a mesh with 52 points, and plotted it on one of the bearing base's xy-surface (Fig. 3.b). To replicate the simulation's boundary conditions (free), the piece was tied to a beam by nylon strings in two of its edge holes, located in the same y-height. The bearing base response was measured by the uniaxial accelerometer model 352C33 from PCB Piezotronics with sensitivity of  $10.38 \pm 10\%$  mV/(m/s<sup>2</sup>) secured with wax on the bearing base's surface. In order to excite the component, we used the impact hammer model 8206 from B&K with aluminium tip and sensitivity ( $< \pm 1\%$ ) 22.7 mV/N. We opted for fixed accelerometer and roving of the hammer.

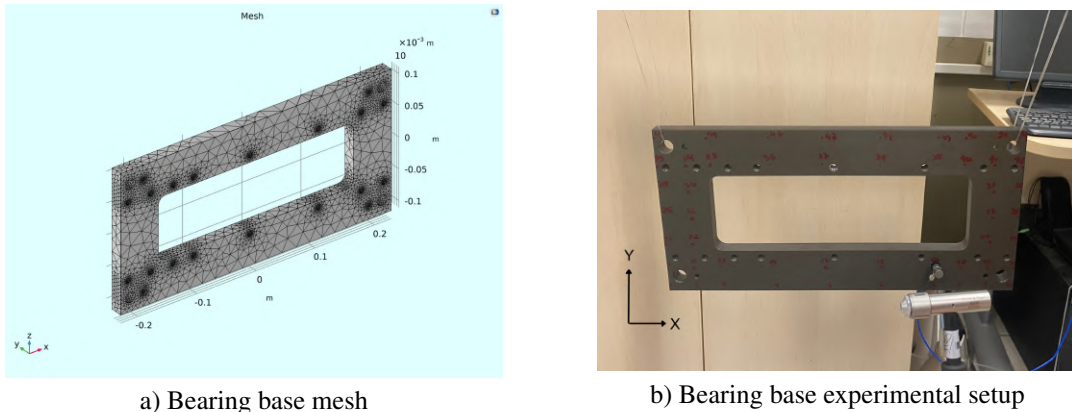


Figure 3. Bearing base's COMSOL Multiphysics mesh and experimental setup

## 3.2 Bearing support

This section presents the experimental and numerical modal analysis methods of the bearing support.

### 3.2.1 Numerical methods

In this FEM modal analysis, we utilized the COMSOL Multiphysics software. We employed the "Free Tetrahedral method" with a custom size to generate the elements for the mesh, where the maximum element size was set to 14.6 mm and the minimum size to 2.63 mm. We achieved (Fig. 4.a) an average element skewness of 0.616. The resulting mesh consisted of 38,710 elements and 7,511 nodes. The boundary conditions were set to Free, maintaining consistency with the experimental setup. To generate an FRF, a unitary harmonic punctual force in the point where the accelerometer was fixed. This FRF was used to compare with the experimental one, then to update material properties of the component. We utilized the "Frequency domain modal solver", identifying the first 18 modes in the analysis, with a frequency range of 1-15000 Hz and a frequency resolution of 1 Hz.

### 3.2.2 Experimental methods

The experimental mesh (Fig. 4.b) was set with 50 points distributed to cover most of the component while avoiding the holes. On the x-axis, they were all separated by 1.5cm on the x-axis. On the y-axis, 7 lines were plotted 1.5cm apart from each other and 2 more lines, 1cm apart from each other. We opted to use a smaller impact hammer, model 086D80 from PCB Piezotronics with sensitivity equal to ( $< \pm 1\%$ ) 22.48 mV/N and aluminum tip, due to the component's higher natural frequencies. We used the same accelerometer as the bearing base analysis, also secured with wax and opted for hammer roving.

## 3.3 C-shaped beam

This section presents the experimental and numerical modal analysis methods of the C-shaped beam.

### 3.3.1 Numerical methods

For the C-shaped beam, we utilized the "Free Tetrahedral method" with custom size to generate the elements for the mesh. The maximum element size was set to 22.3 mm, while the minimum element size was 4.01 mm. We obtained an average element skewness of 0.632. The resulting mesh comprised 12,376 elements and 3,596 nodes (Fig. 5.a). The boundary condition was set to fixed in the xz-plane, simulating the operational configuration. To generate an FRF, a unitary harmonic punctual force in the point where the accelerometer measuring the z-direction was fixed. This FRF

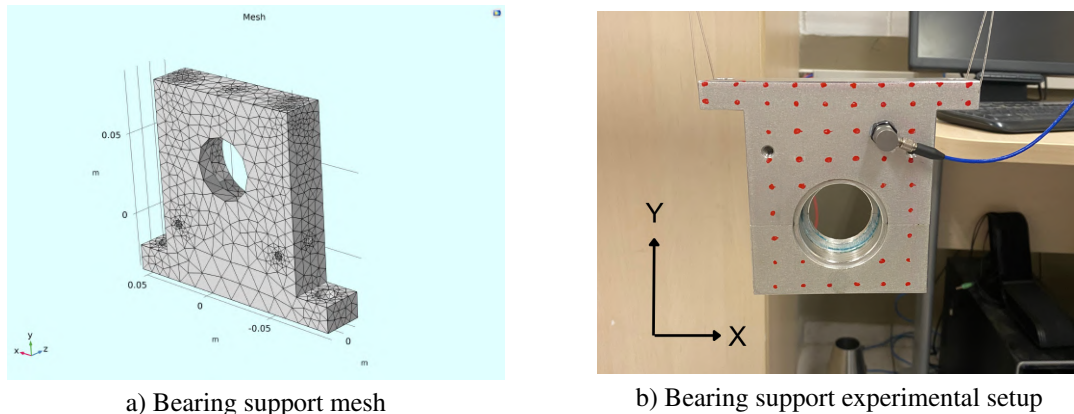


Figure 4. Bearing support's COMSOL Multiphysics mesh and experimental setup

was used to compare with the experimental one, then to update material properties of the component. We employed the “Frequency domain modal solver” identifying the first 18 modes, with a frequency range of 1-3000 Hz and a frequency resolution of 1 Hz.

### 3.3.2 Experimental methods

For the C-shaped beam, we used 72 experimental points, evenly distributed in 8 columns and 6 and 2 lines on the xy and xz surfaces respectively (Fig. 5.b). In order to emulate boundary conditions of the test bench in operation, the beam was fixed by three screws on its base. To capture the response in both planes, we placed one accelerometer at the y-direction and another at the z-direction, models 353B16 with sensitivity ( $\pm 10\%$ )  $1.040 \text{ mV}/(\text{m}/\text{s}^2)$  from PCB Piezotronics and JM353B15 with sensitivity ( $\pm 10\%$ )  $1.053 \text{ mV}/(\text{m}/\text{s}^2)$ , respectively. To excite the component we opted for hammer roving. The impact hammer is model 8206 from B&K with aluminum tip and sensitivity ( $<\pm 1\%$ )  $22.7 \text{ mV}/\text{N}$ .

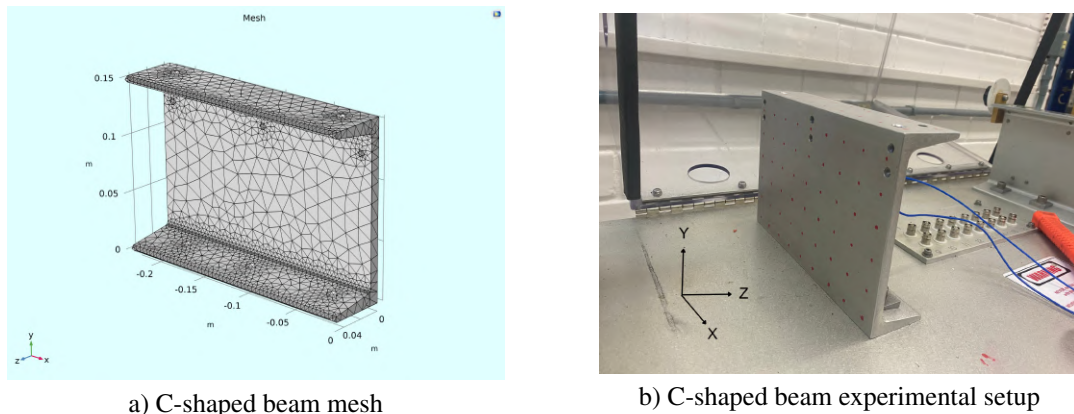


Figure 5. C-shaped beam's COMSOL Multiphysics mesh and experimental setup

## 3.4 Assembly

This section presents the experimental and numerical modal analysis methods of the assembly.

### 3.4.1 Numerical methods

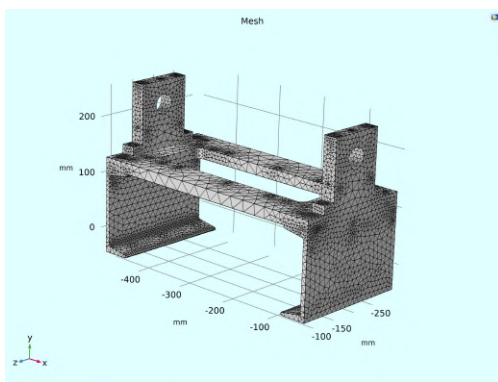
Utilizing the COMSOL Multiphysics software, we initiated the process by creating a mesh of the domain. Our objective was to achieve an average element skewness of over 0.6. We employed the “Free Tetrahedral method” with the default “fine” settings provided by COMSOL Multiphysics. This configuration resulted (Fig. 6.a) in a mesh comprising 136,223 elements and 28,803 nodes, with an average skewness of 0.641.

For this simulation, our boundary conditions were set to “Free”. We used the “Frequency domain modal solver” in order to extract a FRF from our system so we can do a comparison with the experimental data that will be presented in the results section. The applied force corresponded to a unitary harmonic point force at the location where the shaker would be fixed during the experimental analysis. The modal solver setup involved up to 40 modes with a maximum frequency of 3600 Hz. We solved the frequency range from 1 Hz to 1600 Hz with a frequency resolution of 1 Hz.

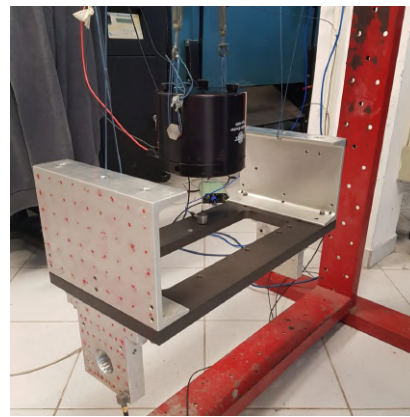
### 3.4.2 Experimental methods

Initially, we attempted the assembly's experimental modal analysis with the C-shaped beams screwed into the main base of SpectraQuest's MFS, emulating operational conditions. However, this test resulted in measurements with significant noise, complicating the analysis. After some investigation, we inferred that the noise came from MFS's whole structural response. In light of this information, we opted to proceed with free-free boundary conditions, limiting the analysis to the investigated components.

We utilized 246 experimental points on the assembly mimicking the point distribution of the individual components' analysis. To manage the increased number of measurements, we decided to employ the excitation of a shaker with accelerometer roving. The assembly was suspended using a steel cable tied to the middle hole of each C-shaped beam (see Fig. 6 b). The shaker was also suspended by steel cables. The shaker, B&K model 4809, was connected to the structure by a stinger. We employed a force transducer from B&K, model 8230-001, with a sensitivity of ( $\pm 1\%$ ) 21.41 mV/N, to measure the force applied on the structure. Since we wanted to capture the movement in all directions, we used two triaxial accelerometers from B&K model 4525-B. These accelerometers have sensitivities ( $\pm 10\%$ ) 1.009 mV/(m/s<sup>2</sup>), ( $\pm 10\%$ ) 1.079 mV/(m/s<sup>2</sup>), and ( $\pm 10\%$ ) 1.039 mV/(m/s<sup>2</sup>) in the X, Y, and Z directions, respectively.



a) Assembly mesh



b) Assembly experimental setup

Figure 6. Assembly's COMSOL Multiphysics mesh and experimental setup

### 3.5 Model adjustment

In the absence of information regarding the specific alloys used in each component of the SpectraQuest's Machine Fault Simulator, we had to resort to measurements in order to define the material parameters. At SolidWorks we were able to obtain the volume of each part. We measured the mass of each component by using a weighting scale. We obtained the density of each component that was used at COMSOL Multiphysics with the volume and mass information.

After obtaining the density and with a visual inspection of the components, we inferred that their material was of an aluminium alloy. At COMSOL Multiphysics, we varied the Young's modulus within the expect range for aluminium alloys. The Young's modulus was determined by comparing simulated and experimental FRFs. The final values for the material proprieties are showed in the Tab. 1. To adjust the structure's damping, we employed the experimental damping ration acquired from BK Connect software. We extracted the value for each mode and inserted in the modal solver of the frequency domain modal solver at COMSOL Multiphysics.

Table 1. Adjusted proprieties of the materials

Component	Density [kg/m <sup>3</sup> ]	Youngs's modulus [GPa]	Poisson's ratio
Bearing Base	2621.4	69	0.33
Bearing Support	2748	56	0.33
C-shaped Beam	2717.7	69	0.33

## 4. RESULTS

This section presents the experimental and numerical modal analysis of the bearing base, bearing support, C-shaped beam and the assembly of these components

#### 4.1 Bearing base

Table 2 shows the bearing base’s experimental (“Exp. [Hz]”) and numerical (“Num. [Hz]”) natural frequencies. The first, second and fourth acquired vibration modes and their frequencies are significantly close to the ones resulting from the numerical simulation, as shown on Tab. 2. A discrepancy between the two frequencies in the third mode may be due to an acquisition error occurring during experiments, such as a possible inadequate accelerometer positioning. At the lower frequencies, experimental and numeric results are close in shape, as shown in Fig. 7.

Table 2. Bearing base’s experimental and numerical natural frequencies

Mode	Exp. [Hz]	Num. [Hz]
1	408	409
2	419	421
3	682	776
4	1166	1167
5	1393	1316

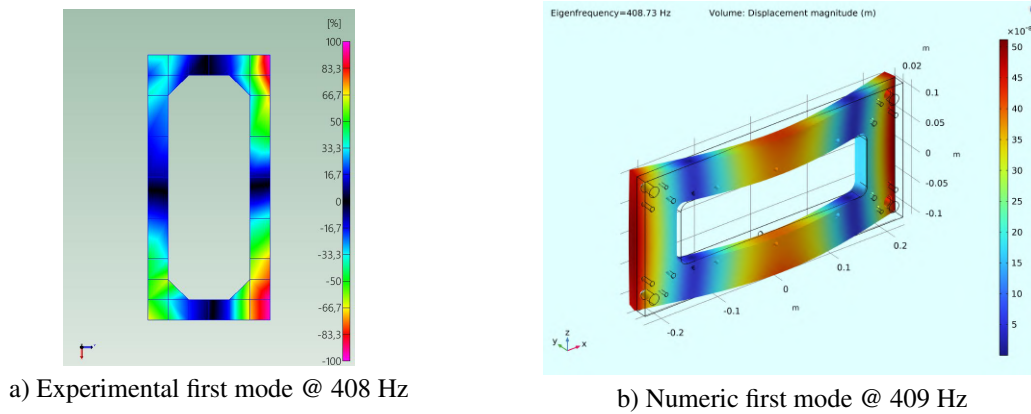


Figure 7. First mode Bearing base comparison

#### 4.2 Bearing support

Table 3 shows the bearing support’s experimental (“Exp. [Hz]”) and numerical (“Num. [Hz]”) natural frequencies. There’s a considerable difference between experimental and numerical natural frequencies. Their associated modes, however, are quite similar. This could be attributed to the fact that the bearing support is not a single piece, but rather a junction of two parts held together by screws, that could be misrepresented on the CAD model. Despite minor deviations observed in some modes, in the third mode in Fig. 8, both the shape and frequency remain virtually unchanged.

Table 3. Bearing support’s experimental and numerical natural frequencies

Mode	Exp. [Hz]	Num. [Hz]
1	3487	3818
2	5605	6244
3	7648	7652
4	8802	8842
5	9455	9565

#### 4.3 C-shaped beam

In the C-shaped beam modal analysis, numerical and experimental methods culminated in close eigenfrequencies (see Tab. 4), along with similar vibration modes as shown on Figs. 9(a) and 9(b). The fifth mode presented the highest deviation among all. Therefore, material properties and boundary conditions were properly modeled in this component.

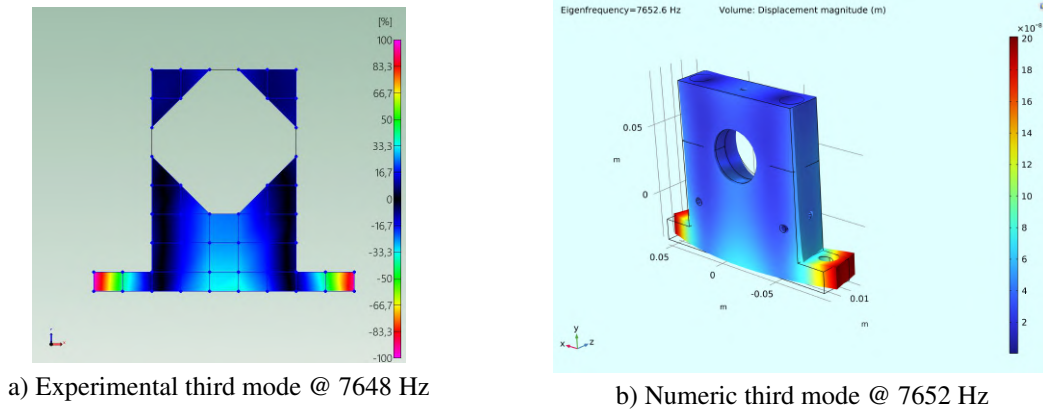


Figure 8. Third mode comparison of the bearing support

Table 4. C-shaped beam's experimental and numerical natural frequencies

Mode	Exp. [Hz]	Num. [Hz]
1	213	220
2	434	438
3	1293	1295
4	1789	1789
5	2606	2557

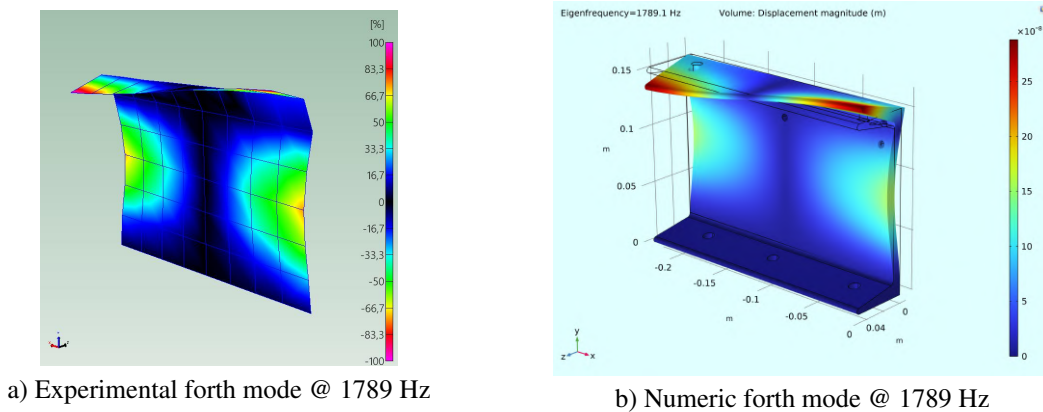


Figure 9. Forth mode comparison C-shaped beam

#### 4.4 Assembly

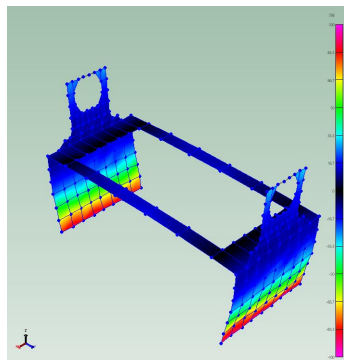
Table 5 shows the bearing support's experimental ("Exp. [Hz]") and numerical ("Num. [Hz]") natural frequencies, demonstrating close agreement between them. Additionally, Fig. 10 illustrate the similarity of modal shapes in both numerical and experimental analyses. In the fifth numerical mode, a symmetric mode was observed as we can see in Fig. 11.

Figure 12 compares the experimental and COMSOL Multiphysics simulation absolute values of the punctual Acceleration in the y-axis. There is a peak around 20 Hz at the experimental curve. Analysing its movement at the BK Connect software, we conclude that it is a mode associated with the experimental assembly frequency. It represents a simple harmonic translation of the whole structure.

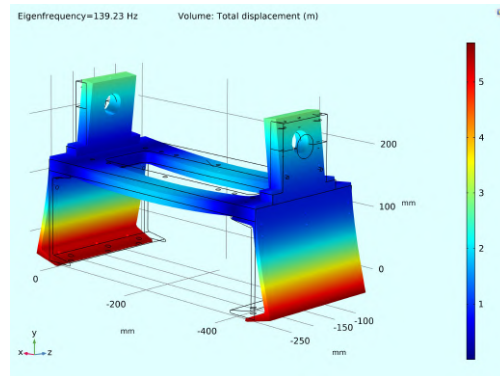
Regarding the shapes of the FRFs at Fig. 12, there's close agreement in the 50-300 Hz range between experimental and numerical results. However, beyond 300 Hz, a difference in line shapes becomes noticeable, even though the eigenfrequencies remain in close proximity. This phenomenon may be attributed to a focused model adjustment in lower frequencies, potentially resulting in differences due to the damping of higher modes due to the complexity and number of joints.

Table 5. Assembly's experimental and numerical natural frequencies

Mode	Exp. [Hz]	Num. [Hz]
1	136	139
2	179	188
3	202	211
4	305	314
5	418	420-423
6	558	563
7	653	633

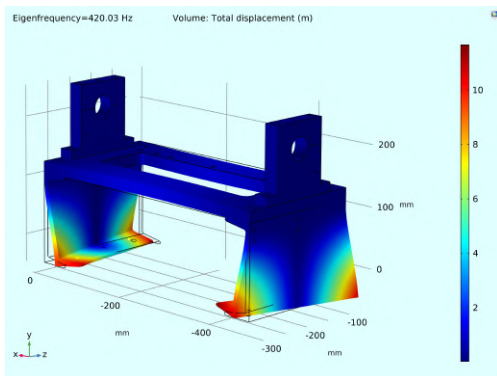


a) Experimental first mode @ 136 Hz

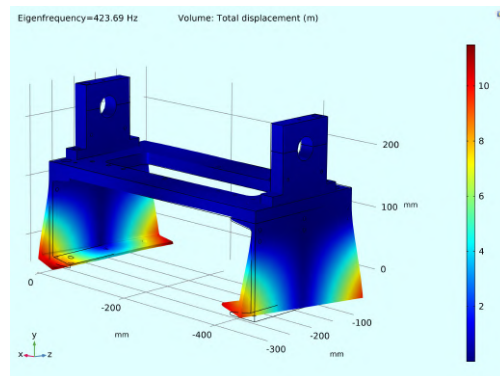


b) Numeric first mode @ 139 Hz

Figure 10. First mode comparison



a) First symmetric mode @ 420 Hz



b) Second symmetric mode @ 423 Hz

Figure 11. Comparison of the symmetric numeric modes

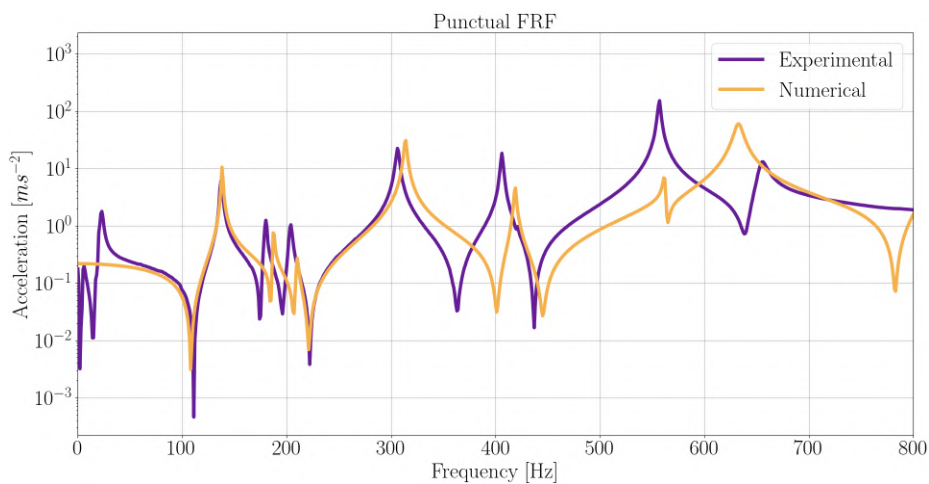


Figure 12. Punctual acceleration in the y-direction

## 5. CONCLUSIONS

This article conducted experimental and numerical modal analyzes of SpectraQuest's *Machinery Fault Simulator* with the objective to describe the dynamic response of the test bench components aforementioned. This was motivated by a need to separate which response to an excitation came from the machine elements or the structure itself. Experimental modal analyses were performed on each component – bearing base, bearing support, C-shaped beam – and their assembly to obtain more accurate material properties. Both experimental and numerical modal analyses were conducted, and damping was adjusted using experimental data processed by BK Connect. The results were incorporated into the FEM model at COMSOL Multiphysics.

The results revealed that the eigenfrequencies exhibited close agreement between the numerical and experimental results, but deviations were observed at higher frequencies. The modal shapes were found to be similar in both analyses. The numerical model is now able to represent the analysed components of MFS's test bench. However, the complexity of certain parts – such as the bearing support with its two separate components and the bolted joints – posed challenges in accurately modeling them at the FEM software. Further analysis of the assembly FRFs indicated that the two curves were close at lower frequencies, but the deviation increased with higher frequencies. This observation was expected due to the complexity and the number of joints involved in the system.

Anticipating future studies, the next step involves refining our model within COMSOL with a specific focus on enhancing the representation of damping and contact interactions between components. These aspects are likely contributors to the observed deviation between the numerical and experimental FRF at higher frequencies. Another essential aspect is the inclusion of bearings and axles in the model, completing the core components of the SpectraQuest's MFS.

## 6. ACKNOWLEDGEMENTS

We thank Dynamox S/A and the Laboratory of Vibrations and Acoustics at UFSC, supported by FEESC, for making this work possible through the project "Technologies for the analysis of noise and vibration signals for the detection, prognosis, and correction of failures in machines and structures.". Special thanks to Olavo M. Silva, which contributed greatly with this work.

## 7. REFERENCES

- Beards, C., 1996. *The vibration of structures with more than one degree of freedom*, Elsevier, pp. 83–128. doi: 10.1016/B978-034064580-2/50005-3.
- Ewins, D.J., 2009. *Modal Testing: Theory, Practice and Application*. Research Studies Press LTD., second edition edition.
- Maia, N.M. and Silva, J.M.M.S., 1997. *Theoretical and Experimental Modal Analysis*. John Wiley Sons.
- Meirovitch, L., 2002. *Fundamentals of Vibrations*. 1st edition. ISBN 0072881801.
- Mustafa, A.M. and Nayfeh, J.F., 2020. "Experimental research on machinery fault simulator (mfs): A review". IEEE, pp. 72–78. ISBN 978-1-7281-5675-0. doi:10.1109/PHM-Besancon49106.2020.00019.
- Petyt, M., 2010. *Introduction to Finite Element Vibration Analysis*. Cambridge University Press, second edition edition. ISBN 978-0-521-19160-9.
- Randall, R.B., 2011. *Vibration-based Condition Monitoring*. Wiley. ISBN 9780470747858. doi:10.1002/9780470977668.
- Rao, S.S., 2010. *Mechanical Vibrations*. Pearson, 5th edition. ISBN 0132128195.
- Shabana, A., 2019. *Vibration of Discrete and Continuous Systems*. Springer, third edition edition. ISBN 978-3-030-04347-6. doi:https://doi.org/10.1007/978-3-030-04348-3.
- SpectraQuest, 2023. "Spectraquest's machinery fault simulator". URL <https://spectraquest.com/machinery-fault-simulator/details/mfs/>.
- Tiboni, M., Remino, C., Bussola, R. and Amici, C., 2022. "A review on vibration-based condition monitoring of rotating machinery". *Applied Sciences*, Vol. 12, p. 972. ISSN 2076-3417. doi:10.3390/app12030972.

## 8. RESPONSIBILITY NOTICE

L. F. R. Fonseca, M. V. Sikora, L. Y. A. Kaneko, J. Cordioli and D. Braga are solely responsible for the printed material included in this paper.